IEEJ Journal of Industry Applications
Vol.8 No.4 pp.608–614 DOI: 10.1541/ieejjia.8.608

Paper

Time Domain Analysis of Transmission Failure on CAN System due to Differential-Mode Noise Emitted from a Buck Converter

Ryo Shirai[*a)] Student Member, Toshihisa Shimizu[*] Fellow

(Manuscript received June 29, 2018, revised Feb. 19, 2019)

The controller area network (CAN) is one of the serial bus systems used in various applications, such as automobiles, airplanes, and industrial robots. This study focuses on analysis of electromagnetic interference (EMI) caused by a buck converter installed close to a CAN bus, and highlights the problems in a conventional EMI evaluation, followed by the development of an experimental EMI mitigation method. The verification experiments show that the periodic switching noise of a buck converter causes data-transmission failure in CAN. Finally, this study proposes a novel control method for a buck converter, which can mitigate EMI in CAN.

Keywords: buck converter, CAN, electromagnetic noise, EMI, spread-spectrum technique

1. Introduction

The electromagnetic interference (EMI) caused by switching converters has always been a problem. Moreover, communication networks such as local area networks (LANs) are one of the remarkable EMI victims. Unintentional EMI noise from a power converter, which propagates as radiation noise or conduction noise, deteriorates signal integrity in communication networks and causes data-transmission failure in such networks [(1)(2)]. To reduce EMI noise, shielding materials and EMI filter circuits are commonly applied to switching converters or communication networks [(3)–(9)]. However, these conventional EMI reduction methods may not be effective in every situation; therefore, an ad-hoc design that is suitable for each specific application/situation is required. In addition, various international standards are set to ensure electromagnetic compatibility (EMC) between the switching converter and communication network. These standards specify the EMI level of switching converters in the frequency domain, and EMI reduction methods are generally applied with reference to these standards in the frequency domain [(10)].

Meanwhile, only a few studies have been published on the EMI reduction with considering the failure mechanism of EMI victims, such as communication networks [(11)(12)]. Furthermore, the mechanism of EMI noise propagation from switching converters to its victim is mostly unknown. To ensure electromagnetic coexistence between a power converter and communication networks, it is necessary to analyze both collectively. The first objective of this paper is to provide a comprehensive analysis of EMI caused by a buck converter installed close to the communication line of a controller area network (CAN). CAN is one of the common automotive LAN standards and is widely used in powertrain and power control systems where high reliability is required [(13)(14)]. Regarding the electromagnetic susceptibility of CAN, some existing studies have considered the EMI of integrated circuits, fast electrical transient, and other similar factors [(15)–(18)]. However, to the best of the authors' knowledge, only a few studies have focused on the periodic switching noise emitted by a switching converter installed close to a CAN communication line. For instance, Ref. (19) described an improved CAN communication protocol against the periodic switching noise of a switching converter; however, the physical mechanism of the EMI caused by the switching converter resulting in CAN communication failure is not clarified. Moreover, changing the well-established CAN communication protocol is not a realistic solution in an actual system. Therefore, the second objective of this study is to propose a more reasonable EMI mitigation method without modifying the CAN communication protocol.

This paper first presents the configuration of an EMI test bench, which is referred to as a noise injection system, that intentionally generates EMI noise in a CAN communication line. This system effectively realizes stable noise injection and ensures appropriate repeatability of the experimental verification process. The step-by-step mechanism of EMI noise propagation is clarified through several experiments using the noise injection system as presented in section 3. Section 4 presents the result of serial bus analysis to evaluate the performance of CAN communication under the EMI noise environment of a buck converter. The signal integrity of a CAN system significantly changes with the input voltage of a buck converter. An experiment is conducted to suppress the EMI noise of a buck converter in the frequency domain by applying only spread-spectrum modulation to the buck converter, as presented in section 5. However, in this method, the data-transmission failure of CAN is not sufficiently suppressed, which suggests that EMI reduction in the frequency domain is not always effective for reducing the data transmission failure of CAN. In section 6, a switching method of a buck converter is proposed, which is verified experimentally. Although the control method effectively reduces CAN

a) Correspondence to: Ryo Shirai. E-mail: shirai-ryo@ed.tmu.ac.jp
* Tokyo Metropolitan University
1-1, Minami-Osawa, Hachioji, Tokyo 192-0397, Japan

errors, the switching frequency and duty ratio are severely limited. To solve this problem, furthermore, an improved control method of buck converter is proposed. Finally, the conclusions of this study are summarized in section 7.

2. Noise Injection System

The noise injection system is designed as an EMI test bench to intentionally inject EMI noise to the CAN bus line. The system consists of a buck converter and a CAN communication system, as indicated in Fig. 1 and Table 1. As shown in Fig. 2, the parallel-shaped DC bus line and antenna-like CAN bus line are very important features in the system. Moreover, the common-mode noise of the buck converter is suppressed as much as possible by removing its ground wire in the system. Owing to these features, differential-mode noise is injected to the CAN bus line by the effect of magnetic coupling between the DC and CAN bus lines, and the parasitic-oscillation current flowing through the DC bus line dominantly produces noise voltage in the CAN bus line [20]–[22].

The topology of a CAN system follows the CAN protocol

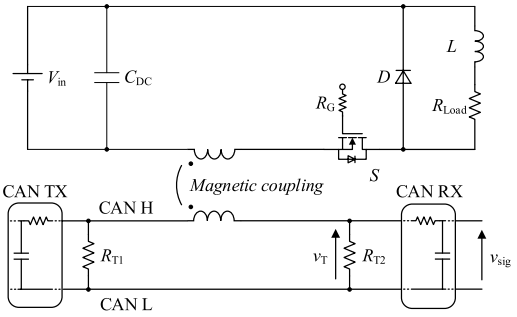

Fig. 1. Equivalent circuit diagram of noise injection system

Table 1. Specifications of the noise injection system

Buck converter	
DC link capacitor C_{DC}	270 µF, DC 400 V_{max} ×2
SiC Schottky diode D	CREE, C3D 10060 A, 600 V, 14.5 A
MOSFET S	Infineon, SPP20N60C3, 650 V, 20.7 A
Inductor L	810 µH
Load resistor R_{Load}	10 Ω
Gate resistor R_G	6.2 Ω
Switching frequency f_S	10–50 kHz (Gate driver: 0 V to 17 V)
Input DC voltage V_{in}	0–200 V

CAN system	
CAN node (TX, RX)	Micro Application Lab. MA 375
Termination resistor R_{T1}, R_{T2}	120 Ω
CAN communication speed	125 kbps
Frame interval	50 ms

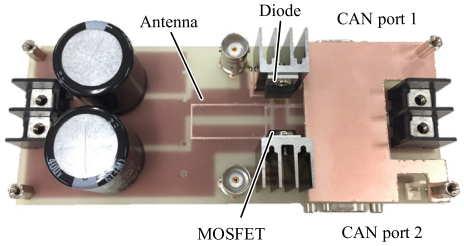

Fig. 2. Photograph of noise injection system

specified by ISO 11898-2, and the communication speed is set to 125 kbps in this study. The rated communication speed of CAN is used from 125 kbps to 1 Mbps. However, CAN errors increase drastically in high speed condition; hence, exploring the CAN failure mechanism caused by EMI noise becomes more difficult compared to low speed condition. In terms of the CAN communication system, two CAN nodes (TX: transmitting node, RX: receiving node) controlled by programmable interface controllers (PICs) are used in its noise injection system and connected accordingly to an antenna-like CAN bus via shielded twisted pair (STP) cables.

3. Mechanism of Noise Propagation from Buck Converter to CAN Bus

3.1 Parasitic-oscillation Waveforms in DC Bus Line

The drain-source voltage v_{DS} of MOSFET when it is turned off is measured because the MOSFET is mounted in the parasitic-oscillation path of the mains circuit. In this study, the parasitic-oscillation current in the DC bus when the MOSFET is turned on is almost negligible since a SiC Schottky diode D is used to suppress the oscillation current as much as possible.

As shown in Fig. 3, a high-frequency damped oscillation waveform appears in the measured voltage waveforms of v_{DS}. These oscillation waveforms are due to the parasitic impedance of the oscillation path. Thus, the parasitic-oscillation waveform in v_{DS} significantly depends on the parasitic impedance of the oscillation path. In addition, the parasitic impedance of the off-state MOSFET affects the oscillation frequency and damping factor of the oscillation waveform [23].

3.2 Noise Propagation in CAN System

The parasitic-oscillation current in the DC bus line is produced when the MOSFET is turned off. Subsequently, noise voltage is induced in the CAN bus line by the effect of magnetic coupling between the DC and CAN bus lines, as shown in Figs. 4(a)–4(d). When the noise voltage is higher than the threshold voltage of the CAN receiver, the signal output voltage drops from 5 V to 0 V, which is defined as the error signal in this study.

In the CAN RX device, a transceiver IC (MCP2551, Microchip Technology Inc.) is used. When noise waveforms are induced in the input terminal of the IC, high-frequency components in the waveforms can be filtered out because the IC has an intrinsic low-pass filter. The intrinsic filter mainly consists of internal parasitic capacitors and resistors in the IC.

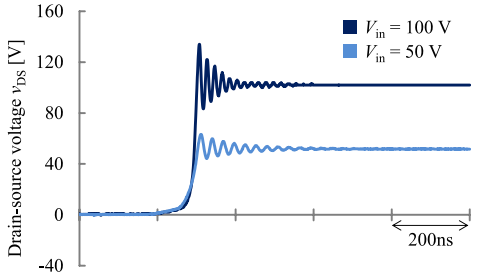

Fig. 3. Measured waveforms of drain-source voltage of MOSFET when V_{in} is set to 50 V and 100 V

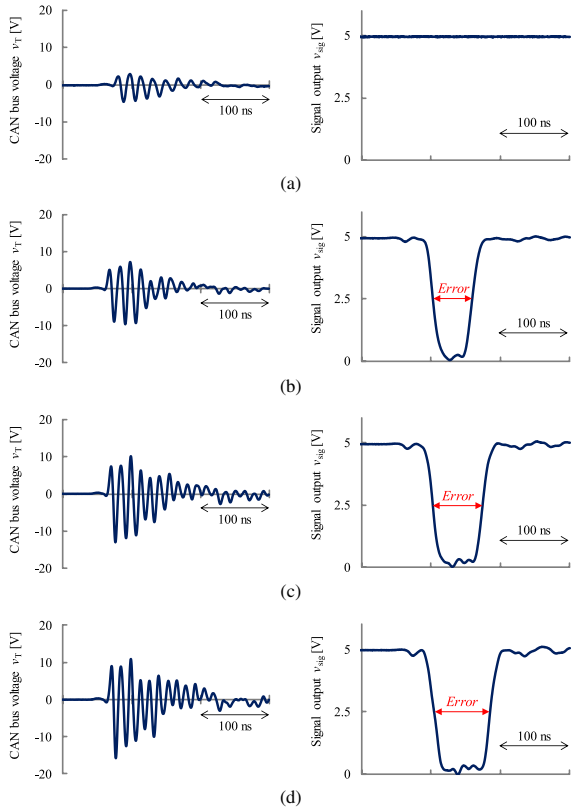

Fig. 4. Measured voltage waveform of CAN bus voltage v_T and signal output v_{sig} when MOSFET is turned off. (a) V_{in} = 50 V, (b) V_{in} = 100 V, (c) V_{in} = 150 V, and (d) V_{in} = 200 V

Thus, it is impossible to observe the actual filtered waveforms because the intrinsic filter is inside the IC package. However, it is expected that the output signal of CAN RX will vary depending on the filtered waveforms and CAN threshold voltage, which is approximately 1 V. Hence, the error signal becomes a single pulse even if the noise voltage has multiple pulses, as shown in Figs. 4(b)–4(d). In addition, the time length of the error signal depends on the noise waveforms.

4. Data-transmission Failure of CAN

The CAN communication process is realized by transmitting data frames at a constant interval. When the EMI noise of a buck converter produces critical error signals in a CAN data frame, the frame fails to transmit its data, which is known as frame loss.

Frame losses occur when noise voltage is induced in a CAN bus voltage v_T and error pulses appear in the signal output v_{sig}. Hence, CAN errors are observed by serial bus analysis under the operation of a buck converter. Serial bus analysis is carried out by varying V_{in} in the range of 0–200 V using a serial bus analyzer (MDO3054, Tektronix, Inc.). The transmitting CAN node continuously transmits data frames to the receiving node at 125 kbps. The frame interval is set at 50 ms and measurement is performed for 2 s. The measured errors are classified as cyclic-redundancy-check (CRC) error, data error, end-of-frame (EOF) error, and frame error, which are detected using the respective functions of the serial bus analyzer.

Figure 5 shows the result of serial bus analysis in the V_{in} range of 0–200 V. The result shows that the overall number of errors gradually increases as V_{in} increases and the time width of the error signal increases. The measurement results indicate that the number of CAN errors is proportional to the total time width of the error signals during one switching period of the buck converter.

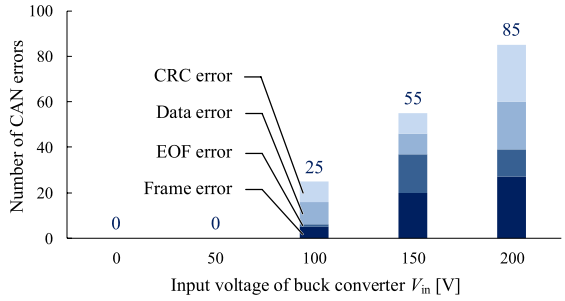

Fig. 5. Measured result of serial bus analysis

5. Effect of Spread-spectrum Modulation Technique on a Buck Converter

Many papers have reported that the noise level expressed by a frequency component is reduced by applying spread-spectrum modulation to a switching converter [24]–[27]. In the case where the switching frequency of the power converter is kept constant, the EMI noise caused by the power converter tends to occur at some specific frequency with relative high noise peak. On the other hand, in the case where spread-spectrum modulation is applied, the EMI noise is distributed to a wide frequency range, and the noise peak at a specific frequency is reduced.

However, it is doubtful that the spread-spectrum modulation realizes effective EMI mitigation in CAN communication because the voltage or current amplitude of switching noise is not reduced and the timing of switching noise is diffused. In other words, CAN frame error caused by switching noise may not be reduced even if spread-spectrum modulation is applied to a switching converter because the average number of switching noises per switching period is still the same as that in constant switching frequency operation. Hence, it seems that spread-spectrum modulation is not effective for improving CAN communication performance.

To verify the effectiveness of the spread-spectrum technique for improving the performance of CAN communication, frequency-modulation control is applied to a buck converter in the noise injection system. In this study, the triangular modulation method was employed to incorporate its simplicity to the system [28]. The switching frequency of the buck converter is linearly modulated in the range of 20–50 kHz in a 1.5-ms cycle, as shown in Fig. 6.

The measurement setup is shown in Fig. 7. The vertical near-magnetic field at the center of the DC bus line is measured using a spectrum analyzer with a 10-mm loop antenna probe. The measurement frequency range is 10–100 MHz to observe the spectral characteristic of the parasitic-oscillation current in the DC bus. Figure 8 shows the measurement result of the near-magnetic field of the DC bus line. The result indicates that frequency-modulation control can reduce the EMI noise of a buck converter in the frequency domain compared to constant frequency operation at 35 kHz, which is the

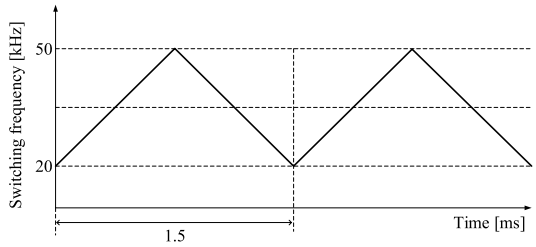

Fig. 6. Modulation pattern of the switching frequency

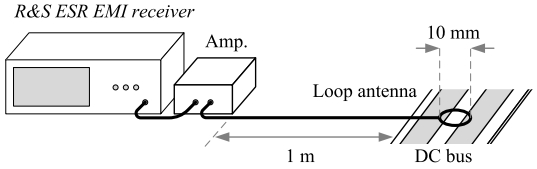

Fig. 7. Measurement setup for spectrum analysis on the vertical near-magnetic field of a DC bus

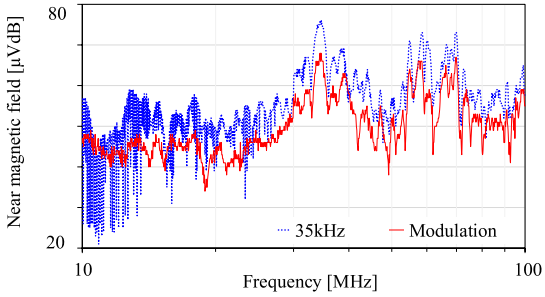

Fig. 8. Measurement result of vertical near-magnetic field at the center of the DC bus

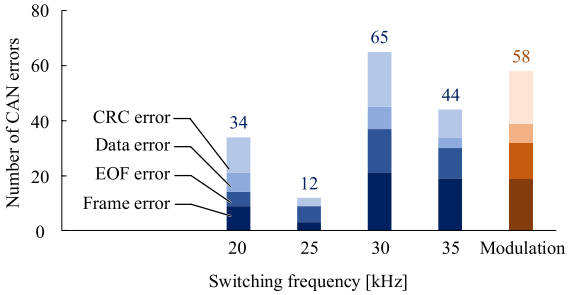

Fig. 9. Measurement result of serial bus analysis

center frequency of spread-spectrum modulation.

Serial bus analysis is carried out while applying frequency modulation control to the buck converter under the same operating condition as measurement of near-magnetic field. Several switching frequencies are used in the range of 20–35 kHz at constant frequency switching conditions for comparison with frequency modulating condition.

As shown in Fig. 9, in the constant switching frequency cases, the number of CAN errors varies depending on the switching frequency. It is considered that the probability of the switching timing and CAN sample timing coinciding may depend on the switching frequency. On the other hand, CAN errors are not sufficiently mitigated compared to those under constant switching frequency conditions even when frequency modulation is applied to the buck converter. It can be expected that the frequency modulation method diffuses the switching timing of the converter, but the probability of both timings coinciding cannot be reduced consistently; sometimes it increases or fortunately decreases depending on the frequency modulating conditions. From the results, the spread-spectrum modulation technique is not a promising method of improving the robustness of CAN communication line against the EMI noise of a power converter.

6. Development of EMI Mitigation Methods Based on Time-domain Analysis

6.1 Basic Mechanism of CAN Communication Failure Figures 10(a) and 10(b) show a simplified schematic waveform of CAN communication signal and noise voltage. When noise voltage is induced on a period other than the CAN bit-sample point, as shown in Fig. 10(a), no error will occur. However, when the timings of the noise voltage and the CAN bit-sample point coincide, as shown in Fig. 10(b), the possibility of CAN signal error is significantly increased. Therefore, matching of the CAN bit-sample point and noise voltage must be avoided to prevent data-transmission failure of CAN communication.

6.2 Development of EMI Mitigation Methods In general, the switching signal of power converters and CAN systems are not synchronized, and switching noise is injected randomly to the CAN systems. Hence, the probability of the noise timing and sample timing coinciding depends on the operating condition. To prevent them from coinciding, the switching timing of the buck converter should be set at the rising timing of the CAN communication signal where it is away from the sample timing. To realize this synchronization, a start-stop synchronization method is employed in the noise injection system.

Figure 11 shows a start-stop synchronization controller (SSC) embedded in the noise injection system. Figure 12 shows the timing chart describing how the SSC operates in the time domain. When the start timing of each frame is transmitted to the CAN bus, the switching timing of the buck converter is re-synchronized with the operating clock of CAN. In this study, the switching frequency of the buck converter is set to 15.125 kHz, which is a quarter of the operating frequency of CAN (62.5 kHz), because the switching frequency must be a common divisor of the operating

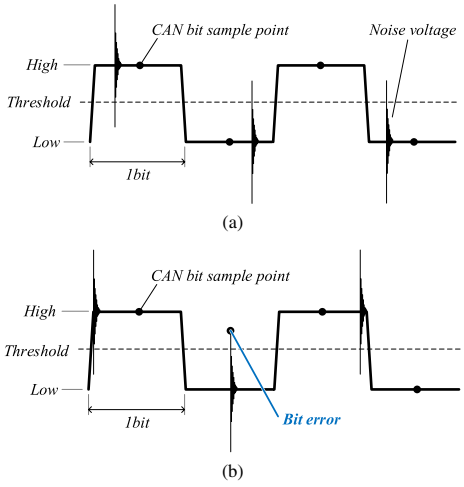

Fig. 10. Simplified schematic waveforms of CAN communication signal and induced noise voltage. (a) No bit errors and (b) with bit error

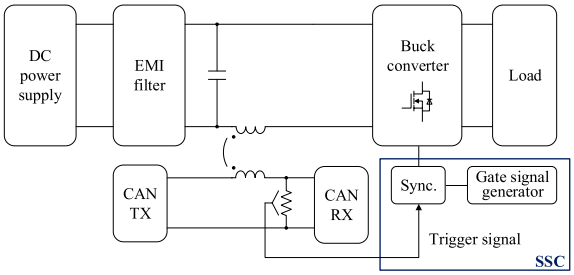

Fig. 11. SSC embedded in noise injection system

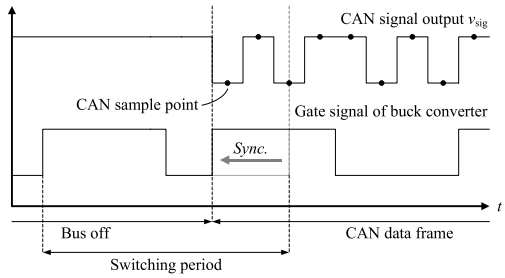

Fig. 12. Timing chart of CAN signal output and gate signal of buck converter when start–stop synchronization is applied

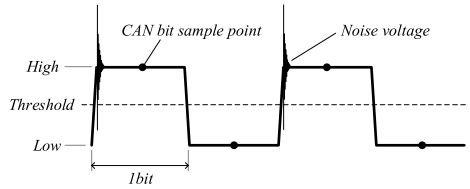

Fig. 13. Schematic waveform of a CAN communication signal and induced noise voltage when start–stop synchronization control is applied

frequency of CAN. The output signal of the CAN receiver is shown in Fig. 13. Noise voltage is simultaneously induced at the timing of the voltage transition of the CAN communication signal, and it never coincides with the CAN bit-sample point.

To verify that the start-stop synchronization control can effectively reduce frame errors in CAN communication, serial bus analysis is carried out while applying start-stop synchronization control to the noise injection system. The result shows that CAN communications are successfully realized, and the frame-error rate is entirely 0%, irrespective of the DC bus voltage V_{in}.

However, there are some drawbacks when start-stop synchronization control is applied. The switching frequency and duty ratio of the buck converter are restricted because the switching timing must coincide with the pulse signal of CAN. This restricts the flexibility of the switching timing of the power converter and affects the control performance.

To solve the problem, an improved method referred to as “timing shift control” is proposed. Figure 14 shows the system configuration of the noise injection system in which a timing shift controller (TSC) is embedded. The TSC consists of a switching hold pulse generator, gate signal generator, and D type flip-flop (D-FF). Figure 15 shows the timing chart of the system. CAN bit sample points are denoted by dots in the CAN signal output waveforms. The switching hold pulse

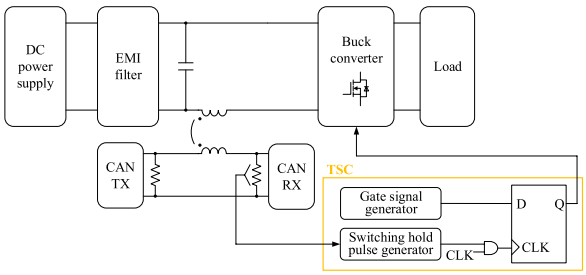

Fig. 14. TSC embedded in noise injection system

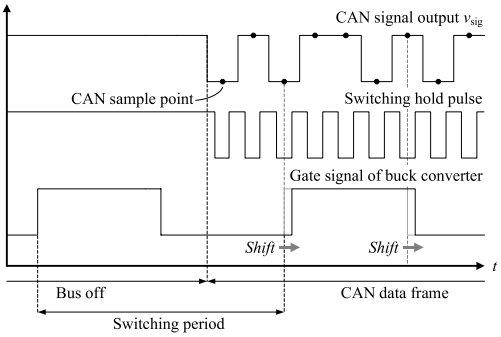

Fig. 15. Timing chart of CAN signal output and gate signal of buck converter when timing shift control is applied

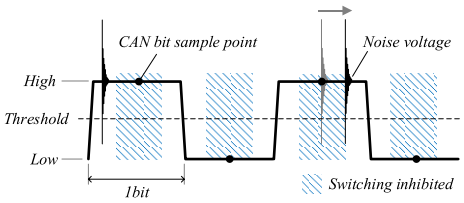

Fig. 16. Schematic waveform of CAN communication signal and induced noise voltage when timing shift control is applied

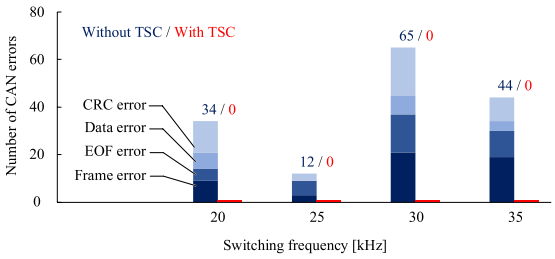

Fig. 17. Measurement result of serial bus analysis with TSC and without TSC

generator outputs a low logic level when the gate signal has to be kept, and the gate signal is held by the D-FF. Hence, the switching action of the buck converter is inhibited during a CAN bit-sample period as shown in the hatched area in Fig. 16, whereas the other period is opened for the switching operation of the buck-converter. Hence, the restriction of switching timing of the buck converter with the SSC is significantly relaxed by the TSC.

To verify the effectiveness of the TSC method, serial bus analysis of CAN communication is carried out in the noise injection system with embedded TSC using a serial bus analyzer. Figure 17 shows the measured result of CAN errors under the operation of the buck converter at several constant

switching frequencies. It can be observed that the TSC successfully avoids CAN errors irrespective of the switching frequency. Hence, the TSC method can be a strong candidate to realize robust operation of CAN system under high EMI noise condition caused by a switching converter.

Although the TSC method is effective for reducing CAN errors, the EMI noise emitted from the buck converter still exists. Hence, combining this method with other reduction methods of EMI emitted from a power converter is necessary to ensure compliance with EMI standards. Further analysis on EMI compliance will be carried out in the future.

7. Conclusions

In this paper, an analysis of EMI caused by buck converters on CAN communication is presented. The measured voltage waveforms in a noise injection system indicate that high-frequency oscillation in the DC bus induces noise voltage in the CAN bus, and noise voltage can cause error signals in the output of the CAN receiver. The results of the serial bus analysis verify that the data transmission failure of CAN communication is significantly affected by the operating condition of the buck converter. Following detailed analysis of the noise injection system, several control methods of the buck converter were experimentally investigated to reduce data transmission failure in CAN communication system. The spread-spectrum technique can effectively reduce the EMI level in the frequency domain. However, the measurement result indicates that it cannot sufficiently reduce data transmission failure in CAN communication. An SSC is proposed and its effectiveness is experimentally verified. When the SSC is applied, the switching frequency and duty ratio were severely limited, although the control method is effective for reducing CAN errors. To solve this problem, the authors also proposed an improved control method of buck converter known as TSC. TSC is effective for realizing the electromagnetic coexistence between the buck converter and the CAN system, and the limitation of the switching timing of the power converter is relaxed compared to SSC.

Acknowledgment

This work was supported by JSPS KAKENHI Grant Number JP16H02328.

References

(1) M. Jin, M. Weiming, P. Qijun, K. Jun, Z. Lei, and Z. Zhihua: “Identification of essential coupling path models for conducted EMI prediction in switching power converters”, *IEEE Trans. Power Electron.*, Vol.21, No.6, pp.1795–1803 (2006)

(2) F. Ren, Y.R. Zheng, M. Zawodniok, and J. Sarangapani: “Effects of electromagnetic interference on control area network performance”, 2007 IEEE Region 5 Tech. Conf., pp.199–204 (2007)

(3) S.C. Tang, S.Y.R. Hui, and H.S.-H. Chung: “Evaluation of the shielding effects on printed-circuit-board transformers using ferrite plates and copper sheets”, *IEEE Trans. Power Electron.*, Vol.17, No.6, pp.1080–1088 (2002)

(4) S. Yang, Q. Chen, and W. Chen: “Common mode EMI noise reduction technique by shielding optimization in isolated converters”, 2016 7th Asia Pacific Int. Symp. Electromagn. Compat. (APEMC), Vol.1, pp.622–625 (2016)

(5) S. Stegen and J. Lu: “Shielding effect of high frequency power transformers for DC/DC converters used in solar PV systems”, 2010 Asia-Pacific Int. Symp. Electromagn. Compat. (APEMC), pp.414–417 (2010)

(6) M. Ali, E. Labouré, F. Costa, and B. Revol: “Design of a hybrid integrated EMC filter for a DC-DC power converter”, *IEEE Trans. Power Electron.*, Vol.27, No.11, pp.4380–4390 (2012)

(7) M. Hartmann, H. Ertl, and J.W. Kolar: “EMI filter design for a 1 MHz, 10 kW three-phase/level PWM rectifier”, *IEEE Trans. Power Electron.*, Vol.26, No.4, pp.1192–1204 (2011)

(8) F.-Y. Shih, D.Y. Chen, Y.-P. Wu, and Y.-T. Chen: “A procedure for designing EMI filters for AC line applications”, *IEEE Trans. Power Electron.*, Vol.11, No.1, pp.170–181 (1996)

(9) H. Tanaka, Y. Saito, H. Kumatani, and T. Azuma: “EMC solution for automotive LAN”, *IEICE Tech. Report*, Vol.104, pp.11–16 (2009)

(10) K. Mainali and R. Oruganti: “Conducted EMI mitigation techniques for switch-mode power converters: A survey”, *IEEE Trans. Power Electron.*, Vol.25, No.9, pp.2344–2356 (2010)

(11) K. Chen, Z. Jin, and H. Chen: “Effect of common-mode interference on communication performance of a motor drive system”, 2016 IEEE Vehicle Power and Propul. Conf. (VPPC), pp.1–6 (2016)

(12) T. Wang, K. Chen, Z. Zheng, and H. Chen: “Modeling and evaluation of common-mode interference coupling effects on sensitive cable in motor drive system”, 2018 IEEE Int. Symp. Electromagn. Compat. and 2018 IEEE Asia-Pacific Symp. Electromagn. Compat. (EMC/APEMC), pp.327–330 (2018)

(13) S. Corrigan: “Introduction to the controller area network (CAN)”, Appl. Report, Texas Instruments, pp.1–15 (2002)

(14) W. Xing, H. Chen, and H. Ding: “The application of controller area network on vehicle”, Proc. the IEEE Int. Vehicle Electron. Conf., 1999. (IVEC ’99), Vol.1, pp.455–458 (1999)

(15) M. Fontana, F.G. Canavero, and R. Perraud: “Integrated circuit modeling for noise susceptibility prediction in communication networks”, *IEEE Trans. Electromagn. Compat.*, Vol.57, No.3, pp.339–348 (2015)

(16) M. Fontana and T.H. Hubing: “Characterization of CAN network susceptibility to EFT transient noise”, *IEEE Trans. Electromagn. Compat.*, Vol.57, No.2, pp.188–194 (2015)

(17) F. Ren, Y.R. Zheng, M. Zawodniok, and J. Sarangapani: “Effects of electromagnetic interference on control area network performance”, 2007 IEEE Region 5 Tech. Conf., pp.199–204 (2007)

(18) M. Fontana, F.G. Canavero, and R. Perraud: “Electromagnetic susceptibility assessment of controller area networks”, Proc. the 2014 Int. Symp. Electromagn. Compat. (EMC Europe 2014), pp.795–800 (2014)

(19) M. Nakamura, M. Ohara, M. Arai, K. Sakai, S. Fukumoto, and K. Wada: “Testbeds of a hybrid-ARQ-based reliable communication for CANs in highly electromagnetic environments”, 2015 IEEE 2nd Int. Future Energy Electron. Conf. (IFEEC), pp.1–6 (2015)

(20) O. Aouine, C. Labarre, and F. Costa: “Measurement and modeling of the magnetic near field radiated by a buck chopper”, *IEEE Trans. Electromagn. Compat.*, Vol.50, No.2, pp.445–449 (2008)

(21) R. Shirai and T. Shimizu: “Basic study of a novel EMC solution for the electromagnetic interference of power converter to CAN”, IEEJ Workshop SPC/MD (2017)

(22) A. Hino, and K. Wada: “Resonance Analysis Focusing on Stray Inductance and Capacitance of Laminated Bus Bars”, *IEEJ J. Industry Appl.*, Vol.5, No.6, pp.407–412 (2016)

(23) K. Kam, D. Pommerenke, A. Bhargava, B. Steinfeld, C.-W. Lam, and F. Centelo: “Quantification of self-damping of power MOSFET in a synchronous buck converter”, *IEEE Trans. Electromagn. Compat.*, Vol.53, No.4, pp.1091–1093 (2011)

(24) R. Mukherjee, A. Patra, and S. Banerjee: “Impact of a frequency modulated pulsewidth modulation (PWM) switching converter on the input power system quality”, *IEEE Trans. Power Electron.*, Vol.25, No.6, pp.1450–1459 (2010)

(25) A. Bendicks, S. Frei, N. Hees, and M. Wiegand: “Systematic reduction of peak and average emissions of power electronic converters by the application of spread spectrum”, *IEEE Trans. Electromagn. Compat.*, No.99, pp.1–10 (2017)

(26) K.K. Tse, H.S.-H Chung, S.Y. Huo, and H.C. So: “Analysis and spectral characteristics of a spread-spectrum technique for conducted EMI suppression”, *IEEE Trans. Power Electron.*, Vol.15, No.2, pp.399–410 (2000)

(27) K. Inoue, K. Kusaka, and J. Itoh: “Reduction in radiation noise level for inductive power transfer systems using spread spectrum techniques”, *IEEE Trans. Power Electron.*, Vol.33, No.4, pp.3076–3085 (2018)

(28) F. Pareschi, R. Rovatti, and G. Setti: “EMI reduction via spread spectrum in DC/DC converters: State of the art, optimization, and tradeoffs”, *IEEE Access*, Vol.3, pp.2857–2874 (2015)

Ryo Shirai (Student Member) received the B.S. degree in Electrical and Electronic Engineering (with highest honor) from Tokyo Metropolitan University, Tokyo, Japan, in 2017. He is currently a master's student at Tokyo Metropolitan University. His research interests include modeling and design of power electronics circuits, and reduction of EMI in power electronics system.

Toshihisa Shimizu (Fellow) received his B.E., M.E. and Dr. Eng. degrees all in Electrical Engineering from Tokyo Metropolitan University in 1978, 1980, and 1991, respectively. He was a visiting professor at VPEC, Virginia Polytechnic Institute and State University, Virginia, USA, in 1998. In 1980, he joined Fuji Electric Corporate Research and Development, Ltd. as a research engineer. Since 1993, he has been with the Department of Electrical Engineering, Tokyo Metropolitan University, Tokyo, Japan. Presently, he is a full professor. His research interests include power converters, high frequency inverters, photovoltaic power systems, modeling and reduction of EMI in power electronics, high power density converter design, and loss characterization of passive components. He is a fellow member of IEEE and a fellow member of IEEJ.